The *Giardia* cell cycle progresses independently of the anaphase-promoting complex

Stéphane Gourguechon*, Liam J. Holt and W. Zacheus Cande

Department of Molecular and Cell Biology, University of California, Berkeley, CA 94720, USA

*Author for correspondence (stephane.gourguechon@berkeley.edu)

Accepted 4 March 2013
Journal of Cell Science 126, 2246–2255

doi: 10.1242/jcs.121632

Summary

Most cell cycle regulation research has been conducted in model organisms representing a very small part of the eukaryotic domain. The highly divergent human pathogen *Giardia intestinalis* is ideal for studying the conservation of eukaryotic pathways. Although *Giardia* has many cell cycle regulatory components, its genome lacks all anaphase-promoting complex (APC) components. In the present study, we show that a single mitotic cyclin in *Giardia* is essential for progression into mitosis. Strikingly, *Giardia* cyclin B lacks the conserved N-terminal motif required for timely degradation mediated by the APC and ubiquitin conjugation. Expression of *Giardia* cyclin B in fission yeast is toxic, leading to a prophase arrest, and this toxicity is suppressed by the addition of a fission yeast degradation motif. Cyclin B is degraded during mitosis in *Giardia* cells, but this degradation appears to be independent of the ubiquitination pathway. Other putative APC substrates, aurora and polo-like kinases, also show no evidence of ubiquitination. This is the first example of mitosis not regulated by the APC and might reflect an evolutionary ancient form of cell cycle regulation.

Key words: Anaphase-promoting complex, APC, Calyculin A, Cyclin B, *Giardia*, Mitosis, Staurosporine

Introduction

Regulation of the eukaryotic cell cycle is mediated in part by signaling cascades orchestrated by protein kinases. Cdk1 (cyclin-dependent kinase 1) and its binding partner, cyclin B, form a complex essential for entry into mitosis (Brizuela et al., 1989; Draetta et al., 1989; Riabowol et al., 1989). Regulation of Cdk1 is achieved by several mechanisms including degradation of cyclin B (Draetta et al., 1989; Whitfield et al., 1990). Cyclin B is targeted for degradation by the proteasome prior to the onset of anaphase by ubiquitin conjugation by the anaphase-promoting complex (APC) (Hershko et al., 1994; King et al., 1995; Yu et al., 1996). Loosely conserved sequences such as D-boxes in the N-terminus of cyclin B have been shown to be necessary and sufficient for recognition by the APC for ubiquitination (Yamano et al., 1998; Geley et al., 2001). Although an APC is present in most eukaryotic lineages its components are not recognizable or are lacking in the Diplomonad and Parabasalid lineages (Eme et al., 2011 and this study).

Giardia intestinalis is a parasitic protozoon that colonizes the small intestine of mammals resulting in maladsorption and diarrhoeal disease (Adam, 2001; Morrison et al., 2007). *Giardia* is a member of the Diplomonads, considered one of the most basal and evolutionary distant eukaryotes (Ciccarelli et al., 2006; Fritz-Laylin et al., 2010) and thus of considerable interest for the study of basic cell biology. It remains unclear if the Diplomonads are part of a group, including the Parabasalids and the Oxymonads (referred to as the POD group), that diverged directly from the last common eukaryotic ancestor (Fritz-Laylin et al., 2010) or if a group termed the Excavates, diverged first then split into several groups including the POD group (Ciccarelli et al., 2006).

The *Giardia* cell cycle is poorly defined at the molecular level with only a handful of proteins identified (Lauwaet et al., 2007; Morrison et al., 2007; Davids et al., 2008; Reiner et al., 2008). By mining the *Giardia* genome database for cyclin homologs (Reiner et al., 2008), several genes have been identified as candidates for a mitotic cyclin on the basis of sequence similarity. Each cell contains two diploid nuclei that are replicated concurrently (Bernander et al., 2001; Sagolla et al., 2006), and then simultaneously segregated to opposite poles of the cell by two separate spindles, prior to cytokinesis (Nohýnkova et al., 2000; Sagolla et al., 2006). Thus, the cell cycle in *Giardia* has G1, S, G2 and M phases similar to other eukaryotes.

In the present study, we show that one of these cyclins, *Giardia* cyclin B, although highly divergent, is required for progression into mitosis. Although *Giardia* has a proteasome (Paugam et al., 2003), and an active ubiquitin conjugation system (Gallego et al., 2007), *Giardia* cyclin B is not regulated by ubiquitin-mediated degradation in contrast to all mitotic cyclins characterized to date. Though *Sacchoromyces cerevisiae* strains have been engineered to complete anaphase and progress to telophase in the absence of an APC (Thornton and Toczyski, 2003) this is the first example of a eukaryotic organism that naturally progresses through the cell cycle without an APC. In *Giardia*, degradation of cyclin B is presumably regulated by interactions with other cell cycle proteins and by phosphorylation. Our findings highlight an evolutionarily distinct cell cycle that uses different regulatory mechanisms in this highly divergent eukaryote.

Results

Giardia cyclin B lacks a degradation motif

Sequence alignment of putative cyclin homologs to cyclins in other organisms shows one of these candidates, *Giardia* cyclin B, has limited sequence (53% similarity in the cyclin box domains) and domain homology to B-type mitotic cyclins (Fig. 1A;

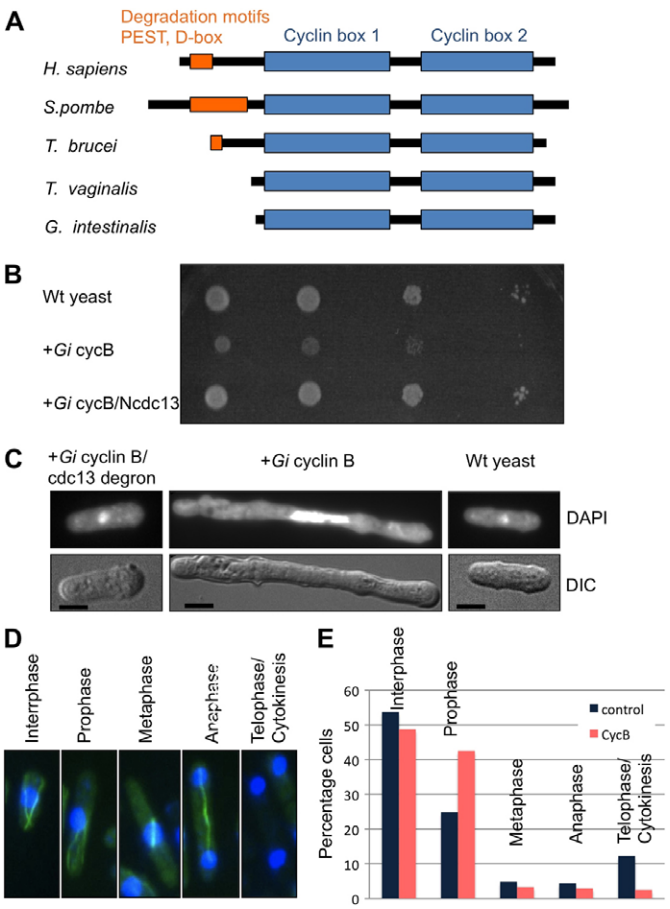

Fig. 1. Toxicity of *Giardia* cyclin B in yeast is linked to its lack of degradation. *Giardia* cyclin B (Accession, GL50803_3977) was expressed in wild-type *S. pombe* cells. Empty vector was used as negative control (Wt yeast). (**A**) Schematic of the sequence alignment of cyclin B from various eukaryotes. Cyclin boxes and degradation motifs are indicated. (**B**) Growth assay of yeast expressing no exogenous protein (Wt yeast), *Giardia* cyclin B (+*Gi* cycB) or *Giardia* cyclin B fused with the degradation signal from the N-terminus of yeast cdc13 (+*Gi* cycB/Ncdc13). (**C**) Morphology of the wild-type yeast and yeast overexpressing *Giardia* cyclin B examined by DIC and DAPI staining. Scale bars: 2 µm. (**D**) Yeast expressing GFP-tubulin were categorized into mitotic subcategories. (**E**) Yeast cells (~500 cells/experiment) expressing no exogenous protein (control) or *Giardia* cyclin B (CycB) were classified into the categories outlined in D and the frequency of each category plotted.

supplementary material Fig. S1). We tagged *Giardia* cyclin B with a triple HA (hemaglutinin epitope) tag and *Giardia* Cdk1 with a triple Myc epitope. We demonstrated that *Giardia* cyclin B co-immunoprecipitates with Cdk1 in *Giardia* (Fig. 2A). In addition after immunoprecipitation and incubation with purified histone H1 and ATP, the *Giardia* cyclin B/Cdk1 shows histone kinase activity (Fig. 2B). No immunoprecipitated histone activity was observed in the absence of cyclin B 3HA expression (Fig. 2B). Taken together, these data suggest *Giardia* cyclin B associates with Cdk1 and is a mitotic cyclin.

To determine if this gene was a mitotic cyclin we assayed its function in fission yeast *S. pombe* by determining whether it could complement a temperature sensitive mutant of the single essential mitotic cyclin cdc13p (Marks et al., 1986). *Giardia* cyclin B could not support fission yeast growth at the restrictive temperature. However expression of *Giardia* cyclin B adversely affected cell growth in wild-type yeast strains (Fig. 1B). Yeast cells expressing *Giardia* cyclin B were elongated, with notably enlarged nuclei (Fig. 1C); these results suggest chromosomes were replicated but failed to properly segregate. We used a strain expressing GFP–tubulin, to visualize mitotic spindles and classify cells into interphase, prophase or cytokinesis (where no mitotic spindle could be seen) and metaphase or anaphase (where the mitotic spindle was visible, as shown in Fig. 1D) and each category quantified (Fig. 1E). A marked increase in the percentage of prophase cells was observed upon expression of *Giardia* cyclin B. Since our results suggest chromosomes can replicate but not segregate after 2–3 days (Fig. 1C) we postulate that *Giardia* cyclin B acts as a dominant negative mutant when expressed in yeast, allowing DNA replication but inhibiting progression into anaphase. Expression of a non-degradable form of cyclin B in yeast leads to inhibition of anaphase progression (Yamano et al., 1996). The phenotypes we observe when *Giardia* cyclin B is overexpressed in fission yeast are slightly different in that cells are arrested before metaphase. These differences may be due to differences between *Giardia* and fission yeast mitotic cyclins. We were not able to detect binding of *Giardia* cyclin B to yeast cdc2 (*S. pombe* Cdk1) by immunoprecipitation suggesting that the cyclin–Cdk interaction is weak or that *Giardia* cyclin B is operating independently of cdc2 in this experiment. Though divergent eukaryotes such as *Trypanosoma brucei* retain an N-terminal degradation motif, neither *Giardia* nor *Trichomonas vaginalis*, a member of the Parabasalids, a sister group to *Giardia*, appear to have N-terminal degradation motifs (Fig. 1A). To test the hypothesis that *Giardia cyclin B* was accumulating improperly when expressed in fission yeast, leading to toxicity, the cdc13p N-terminal degradation motif was inserted upstream of the *Giardia* cyclin B. This chimeric protein, when expressed in fission yeast, did not inhibit yeast cell growth or cause any changes in yeast cell morphology (Fig. 1B,C). There are several possibilities to account for the toxic effects caused by *Giardia* cyclin B expression in *S. pombe*. *Giardia* cyclin B could be binding and irreversibly activating Cdc2. In this scenario cells would arrest because a decrease in Cdc2 activity is required for mitotic progression but *Giardia* cyclin B cannot be degraded. However, the cyclin–Cdc2 interaction must be low affinity since we do not detect an interaction between these two proteins by co-immunoprecipitation. Alternatively, *Giardia* cyclin B could be binding to another yeast cell cycle protein that regulates the Cdc2/Cdc13 complex, such as the Cdk1 inhibitor Rum1, and interfere with its function, thus causing the mitotic block we observe. In conclusion, *Giardia* cyclin B's lack of a degradation motif causes it to inhibit mitotic progression when expressed in fission yeast.

Depletion of cyclin B in *Giardia* impairs cell cycle progression

To investigate the function of *Giardia* cyclin B we used a *Giardia* cell line carrying a 3HA tagged allele of cyclin B (Gourguechon and Cande, 2011) and morpholino-mediated gene specific knockdown (Carpenter and Cande, 2009). Morpholino directed against the cyclin B mRNA efficiently reduced the levels of *Giardia* cyclin B to ~40% after 24 hours (Fig. 3A,B), where this population average represents a subset of cells with very significant depletion (Fig. 3D) and some cells with no depletion.

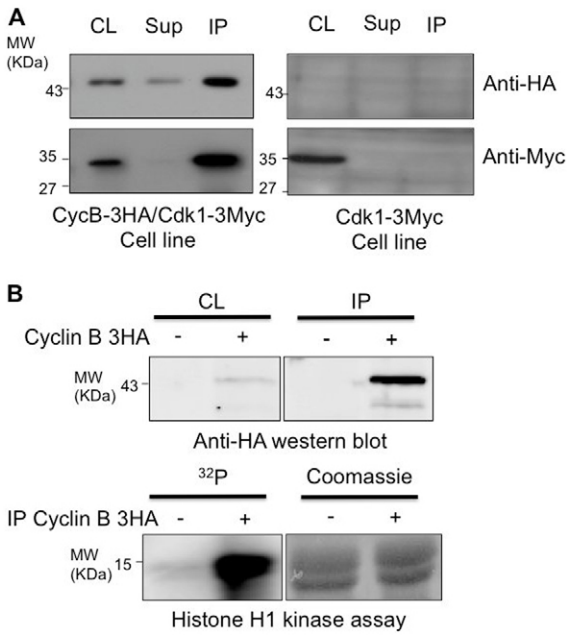

Fig. 2. Cyclin B and Cdk1 interact in *Giardia* cells. (**A**) Cells expressing cyclin B-3HA and Cdk1-3Myc (Accession, GL50803_8037) or cells expressing Cdk1-3Myc only (as indicated) under their native promoters were lysed under non-denaturing conditions. Lysates were incubated with anti-HA agarose (Sigma) for 2 hours at 4°C, washed extensively with PBS then boiled in sample buffer and analyzed by anti-Myc and anti-HA western blotting to probe for Cdk1 or cyclin B, respectively. CL, cleared lysate; Sup, fraction not bound to the beads; IP, immunoprecipitated fraction. (**B**) Cyclin B 3-HA was purified by immunoprecipitation as before, then incubated with histone H1 and [^{32}P]-ATP. Labeling of histone was visualized by autoradiography (^{32}P). Samples were also stained with Coomassie Blue to verify equal loading of histones.

Depletion of cyclin B reduced the cell number by 60% (Fig. 3C); this reflects a mixed population of cells totally depleted of cyclin B, which do not grow, and unaffected cells growing at normal rates. In contrast, mismatched morpholino oligos had no effect on *Giardia* cyclin B levels. Depletion of cyclin B levels also reduced the levels of mitosis-specific, MPM2-antibody positive bands (Fig. 3B) by ~60% compared with the mismatch oligo control. The MPM2 antibody recognizes substrates (phosphoT-P-L-K/Q) phosphorylated during mitosis and is thus an indicator of mitotic progression (Westendorf et al., 1994).

Depletion of cyclin B (as judged by loss of immunofluorescence signal) caused notable morphological changes; chromosomes in cyclin B depleted cells were more condensed (Fig. 3D). In certain cells, we could count 10 chromosomes per nuclei, corresponding to two sets of the replicated *Giardia* chromosomes. Secondly, cells depleted of cyclin B were enlarged (Fig. 3D) compared to control cells transfected with the mismatch morpholino (Fig. 3E). Additionally, large-sized cells were entirely devoid of cyclin B signal (Fig. 3E). Finally cyclin B depleted cells never formed spindles (supplementary material Fig. S2, no spindles in >1,000 cells, compared to 2% in control cells). In *Giardia* cells that were proceeding through anaphase, tubulin immunostaining revealed two mitotic spindles surrounding the two pairs of nuclei as they are segregated towards opposite poles of the cell (supplementary material Fig. S2, mitotic cell). Our results in *Giardia* are similar to those observed in most organisms, where depletion of mitotic cyclins prevents formation of the mitotic spindle and progression into metaphase and anaphase; the only exception is that chromosome condensation still occurs in *Giardia* even when cyclin B is depleted (Booher and Beach, 1988; Riabowol et al., 1989). Thus we conclude that depletion of cyclin B prevents *Giardia* cells from entering mitosis and causes chromosome condensation and cell enlargement.

Cyclin B levels vary during the *Giardia* cell cycle

Having shown that cyclin B is essential for mitotic entry in *Giardia*, we wanted to know whether cyclin B levels vary during the cell cycle, thus showing typical cyclin behavior. We were unable to synchronize and release *Giardia* cells sufficiently to accurately measure the cyclin B levels during the cell cycle, therefore we performed a cell cytometry assay for cyclin B levels, by measuring protein and DNA levels for each individual cell, using immunofluorescence and the CellProfiler program (Carpenter et al., 2006). Cells were categorized into G1, S or G2/M phases of the cell cycle on the basis of nuclear DNA content (Fig. 4A), then quantified for cyclin B 3HA staining (Fig. 4B). This single-cell analysis allowed us to track cyclin B levels during the cell cycle in an asynchronous cell population. As previously described, most of the cells were in the G2/M phase (Fig. 4A) of the cell cycle (Poxleitner et al., 2008; Reiner et al., 2008). The levels of cyclin B 3 HA staining in wild-type, untransfected cells were used to define background levels of fluorescence (Fig. 4C). The mean value of cyclin B staining was then determined for G1, S and G2/M cyclin B 3HA expressing cells, as well as untransfected cells (Fig. 4D). G1 cells (representing 15% of total cells) had low cyclin B levels similar to background levels (Fig. 4B,C). Both S phase cells (43% of total cells) and G2/M cells (42% of total cells) showed a four- and fivefold increase, respectively, in staining for cyclin B (Fig. 4D) compared to levels observed in G1 cells. Thus, we conclude that the levels of cyclin B oscillate during the cell cycle, increasing in S-phase, persisting in G2/M, and returning to low levels before G1, suggesting cyclin B is degraded during mitosis. Consistent with this model, cells in anaphase or cytokinesis (representing 1–2% of the total cell population) generally showed little or no cyclin B staining (supplementary material Fig. S3), when compared to a cell in G2, which shows visible amounts of cyclin B in the cytoplasm. This sudden four- to fivefold decrease in cyclin levels is inconsistent with a model in which cyclin levels are reduced by dilution due to cell growth and suggests a tight temporal control of protein synthesis and/or degradation rates.

To discriminate between transcriptional and post-transcriptional differences we replaced the cyclin B open reading frame with green fluorescent protein (GFP) and analyzed GFP fluorescence versus DNA content by cytometry. Again, cells were classified into G1, S and G2/M according to their DNA content and their GFP content quantified (supplementary material Fig. S4A,C). In contrast to a previous report suggesting cyclin B was regulated at the transcriptional level (Reiner et al., 2008), we observed no notable difference (8.4% change between G1 and G2/M) in GFP levels in G1, S or G2/M cells (supplementary material Fig. S4A,D), suggesting that there was little change in cyclin B promoter activity. In contrast, when expressed using an exogenous, tetracycline-inducible promoter (NlopCycB 3HA), cyclin B levels oscillated during

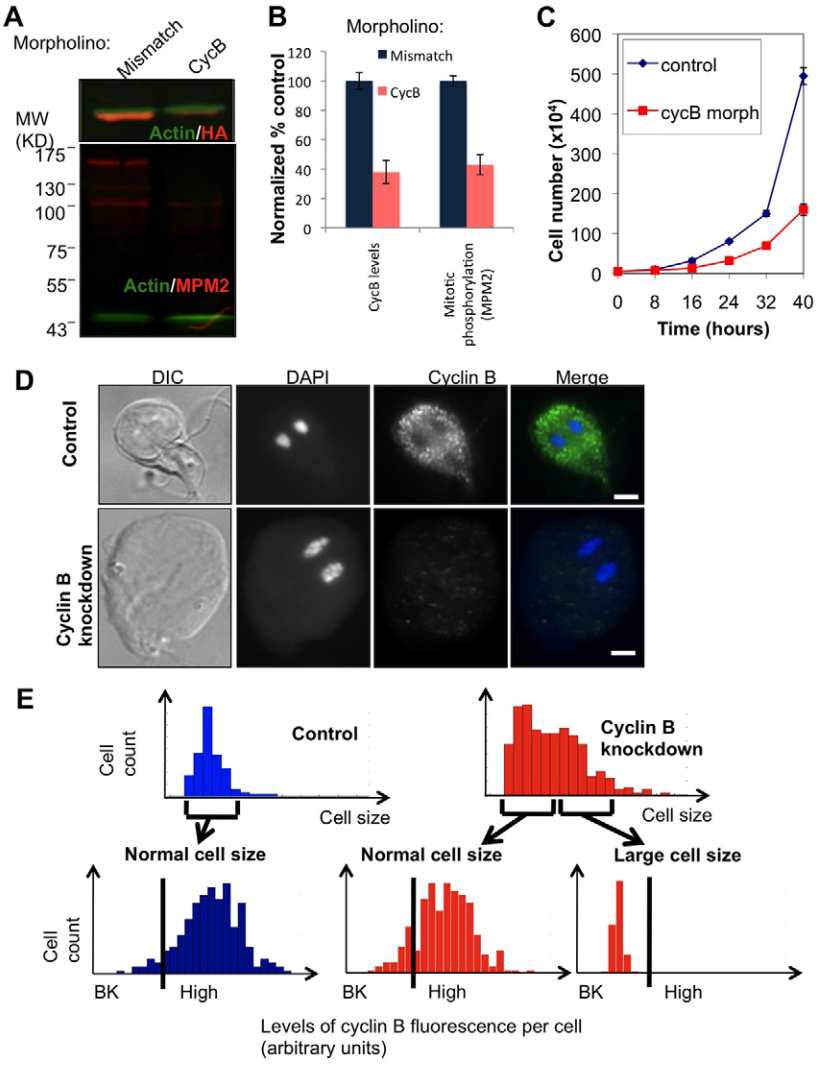

Fig. 3. Depletion of cyclin B in *Giardia*. (**A**) Cells were transfected with anti-cyclin B morpholinos or mismatched morpholino (mismatch) as a negative control. 24 hours after transfection, cells were harvested and analyzed by quantitative western blotting. The signal was visualized and quantified using an Odissey scanner and software (Li-Cor); pseudocolors correspond to the antibodies used, as indicated. The MPM2 antibody, which recognizes proteins phosphorylated during mitosis, was used to quantify entry into mitosis; actin was used as loading control. (**B**) The signals from A were normalized against the actin signal and plotted. (**C**) Growth of control and cyclin-B-depleted cells was monitored every 8 hours and results plotted against time. (**D**) Localization of cyclin B in control (untransfected cells) and cyclin B knockdown cells. An unusual cell morphology and size was observed when cyclin B levels were reduced. Scale bars: 2 µm. (**E**) Sizes of the control cells and cells treated with cyclin B morpholino were determined using the CellProfiler program. Histogram of cell size for the two populations is shown. Cells were further subdivided into cells of normal size (reflecting the size of >99% of untreated cells) and large size (<1% occurrence in normal cells) and the cyclin B signal in each of these cell categories plotted as a histogram. Cells not carrying any 3HA-tagged proteins were used to define background (BK) signal.

the cell cycle in a pattern similar (low levels of cyclin B in G1 cells, 2.5-fold higher levels in S cells and threefold higher levels G2/M cells) to that observed in Fig. 3 (supplementary material Fig. S4B,D). The results suggest that regulation of cyclin B is predominantly post-transcriptional.

Giardia cyclin B is not ubiquitinated

Despite the considerable divergence observed in primary sequence, APC-mediated ubiquitination and degradation of cyclin B has been observed in animals (Yu et al., 1996; Geley et al., 2001), yeast (Yamano et al., 1998), and protozoa such as *T. brucei* (Hammarton et al., 2003; Li et al., 2003). In addition to mediating cyclin B degradation, the APC is responsible for the turnover of other regulatory components such as the polo-like kinase (PLK), aurora kinase (AUK) and Securin. Exhaustive mining of the *Giardia* genome database failed to identify any of the highly conserved components of the APC (Fang et al., 1999; Peters, 2006) such as Apc1-11, and phylogenomic analysis of APC components in multiple eukaryotic lineages show that *Giardia* and *Trichomonas* either lack an APC or it is so highly diverged as to be unrecognizable (Eme et al., 2011). Moreover, we were only able to identify two APC subunits (Doc1 and Cdh1) in *Trichomonas vaginalis*, but we could identify all the previously characterized APC subunits in *Trypanosoma brucei* (Kumar and Wang, 2005). This raised the possibility that cyclin B in *Giardia* is regulated independently of ubiquitin conjugation and the APC. To test these hypotheses, the proteasomal inhibitor MG262 was used to promote enrichment of poly-ubiquitinated proteins in cells carrying 3HA tagged cyclin B, Aurora kinase (AUK) or Polo-like kinase (PLK) which are substrates of the APC in other eukaryotes. Poly-ubiquitinated proteins were further enriched using a ubiquitin-specific affinity matrix (Fig. 5A). Although MG262 promoted the accumulation of poly-ubiquitinated bands (Fig. 5A), it did not immediately halt cell growth, but became toxic after 24 hours (about two cell cycles, Fig. 5B). In contrast, addition of aphidicolin, which blocks DNA replication, immediately and persistently halted cell growth (Fig. 5B).

Upon addition of MG262 and purification of ubiquitin-conjugated proteins, we did not observe any enrichment of our candidate APC substrates (cyclin B, PLK, AUK). We also did not detect any higher molecular weight versions of cyclin B, PLK or AUK, despite the considerable enrichment of poly-ubiquitinated proteins (Fig. 5A). In a separate experiment, we also immunoprecipitated the 3HA-tagged cyclin B, PLK and AUK after addition of MG262 and could not detect any higher

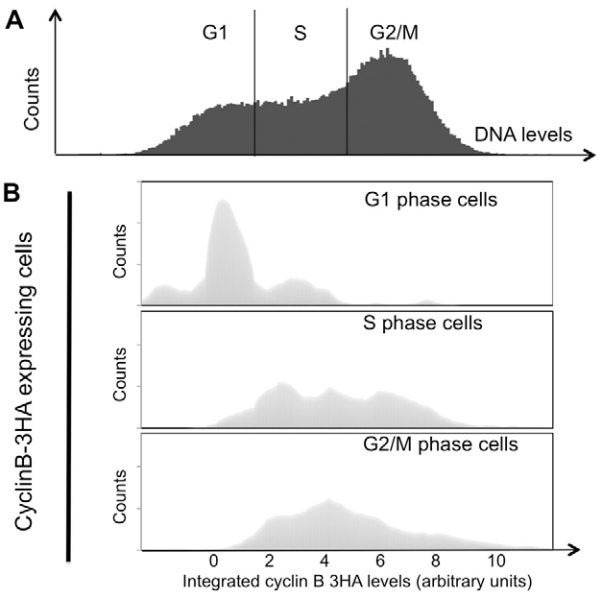

D

Cell type and stage	G1 cells, cycB 3HA	S cells, cyc B 3 HA	G2/M cells, cyc B 3HA	Wt cells, background
Mean Fluoresc. (Arb U)	1.02	4.61	5.07	0.00

Fig. 4. Cyclin B levels oscillate during the *Giardia* cell cycle. (**A**) DNA content of an asynchronous population carrying a 3HA-tagged allele of cyclin B. Histogram of DNA content is shown. (**B**) The same population as A was analyzed, using the CellProfiler program, for their integrated intensity of both DNA and cyclin B. Cells were categorized into G1, S or G2/M and then a histogram for the levels of cyclin B 3HA per cell was plotted using the same scale for all categories. (**C**) Cells not transfected were used to define background levels and data was analyzed as in B. (**D**) Mean values for fluorescence of all indicated cell types.

molecular weight products by western blotting (data not shown). Taken together these data suggest none of our candidate APC substrates were ubiquitinated or conjugated to other small proteins. These results are also inconsistent with the possibility that they undergo sumoylation for the purpose of proteasome-mediated degradation. The absence of an immediate effect on cell growth upon proteasome inhibition by MG262 supports our model that a pathway independent of ubiquitin conjugation degrades cyclin B. In other eukaryotes, such as *T. brucei*, addition of proteasome inhibitors causes an immediate cell growth defect and cells were generally arrested in G2/M (Mutomba et al., 1997). In *Giardia*, even though growth of cells is delayed after 24 hours, there is no immediate mitotic arrest, as cells are still capable of entering anaphase (Fig. 6A).

To investigate the stability of *Giardia* cyclin B we tagged this protein with the SNAP tag (Regoes and Hehl, 2005) to allow *in vivo* labeling of the protein with fluorescein, followed by pulse chase with a non-fluorescent label to determine the decay rate of cyclin B. In our experiments using asynchronous, exponentially growing cells (division time in this experiment was 14.1 hours), cyclin B had a half-life of 8.8 hours (Fig. 5D); consistent with our data, addition of the proteasomal inhibitor MG262 did not alter the half-life of *Giardia* cyclin B (Fig. 5C,D). Our data also suggests that *Giardia* cyclin B is actively degraded, rather than being simply diluted by half after each cell cycle (see theoretical curve for a protein with a 14.1 hour half-life on Fig. 5D). This is further supported by the observation that whereas cells in G2 have visible cyclin B staining (supplementary material Fig. S3) cells that progress into anaphase or cytokinesis (as determined by the segregation of nuclei and morphology) lack any appreciable cyclin B levels, suggesting an active degradation of cyclin B during the metaphase to anaphase transition. These data suggest that inhibiting the proteasome in *Giardia* has no immediate effect on the cell cycle, since cyclin B degradation, and thus mitotic progression is independent of the proteasome and of ubiquitination.

Degradation of *Giardia* cyclin B is regulated by phosphorylation

Since *Giardia* cyclin B is degraded during mitosis by an APC and ubiquitin independent mechanism, we investigated the potential role of phosphorylation. The kinase inhibitor staurosporine and the phosphatase inhibitor calyculin A adversely affected cell growth within 24 hours of addition. Although both these inhibitors have broad specificity, other more specific inhibitors, such as the Cdk/MAPK specific inhibitor roscovitine or the phosphatase inhibitor okadaic acid did not have any appreciable effects on *Giardia* cells. Drug-treated cells were stained for localization of tubulin and actin to further characterize their effects. The proteasomal inhibitor MG262 had no discernible effect after 15 hours on cell morphology or on cell cycle progression (Fig. 6A). Calyculin A appears to inhibit mitosis and cytokinesis, since many multinucleated cells were observed (Fig. 6A), some with multiple mitotic spindles (25% of cells showing spindles, Fig. 6B). In contrast, cells treated with staurosporine failed to enter mitosis, as determined by their inability to form spindles (no cells with spindles, compared to 3% in DMSO-treated cells, Fig. 6B) and the loss of MPM2 specific signal by western blot (Fig. 6C). Additionally, these cells frequently (38%) showed condensed chromatin (Fig. 6A), similar to the cyclin B depleted cells (Fig. 3D), though, unlike cyclin B depleted cells, the cell size was normal. Thus, we conclude that staurosporine prevents cells from entering mitosis, whereas calyculin A inhibits mitotic exit. Using the cyclin B stability assay described, both staurosporine and calyculin A reduced the rate of cyclin B degradation, increasing its half-life to 23.4 and 38.7 hours respectively (Fig. 7A,B).

To test whether calyculin A and staurosporine stabilize *Giardia* cyclin B by altering its phosphorylation, we immunoprecipitated cyclin B from treated cells and analyzed cyclin B by western blot using anti-phosphothreonine antibodies. No HA- or phosphospecific bands were observed when cyclin B was absent (Fig. 8A). When cyclin B was purified, several phospho-specific bands were observed, though none overlapped with the HA-specific cyclin B band (Fig. 8A). These bands probably represent phosphorylated proteins that interact with cyclin B. Staurosporine reduced the number and intensity of these bands when compared to calyculin A treated cells. We are currently characterizing these cyclin B interacting proteins to

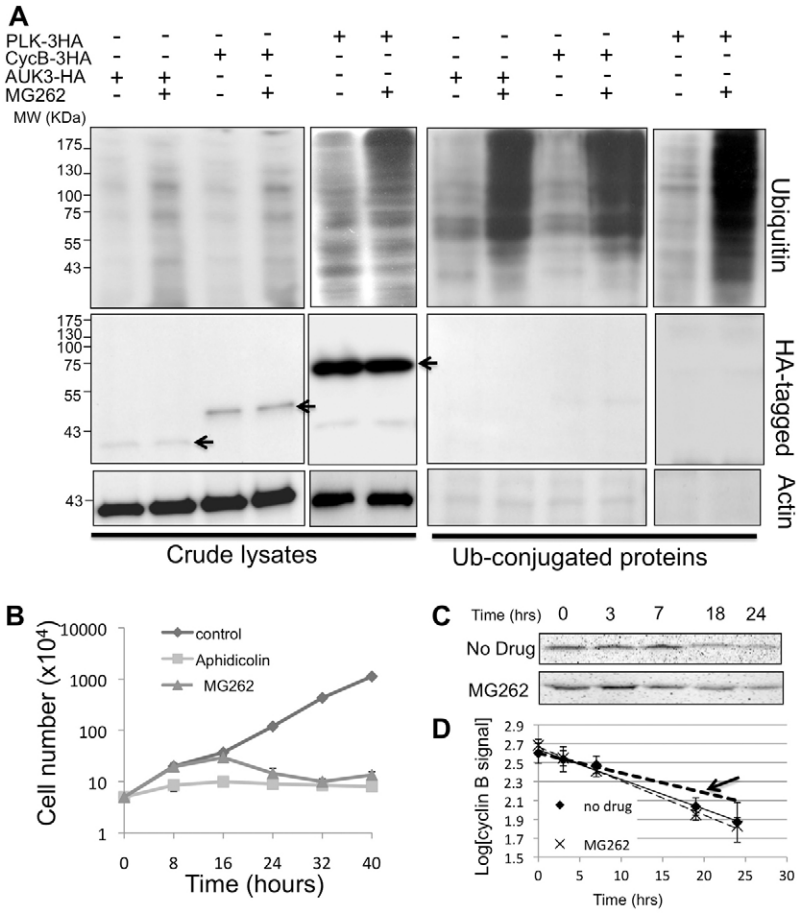

Fig. 5. Presumed APC substrates are not ubiquitinated. (**A**) Cell lines carrying a 3HA-tagged allele of cyclin B (CycB), polo-like kinase (PLK) or aurora kinase (AUK) were incubated with the proteasomal inhibitor MG262 (5 μM, 12 hours) and lysed. Ubiquitin-conjugated proteins were purified from the lysate then probed with anti-ubiquitin antibody; anti-HA was used to detect cyclin B, AUK and PLK. Blots were also probed with anti-actin to ensure equal loading and adequate purification of ubiquitin-conjugated proteins. Arrows indicate the migration of the full-length proteins. (**B**) *Giardia* cells were incubated with 5 μM DMSO (control), 5 μM aphidicolin or 5 μM MG262, as indicated. Cells were counted every 8 hours and the number of cells plotted versus time. (**C**) Cells expressing SNAP-tagged cyclin B were labeled with SNAP-fluorescein, then incubated in the presence or absence of 5 μM MG262. After the indicated time, cells were lysed and the fluorescence quantified. (**D**) Fluorescent signals from duplicates were log transformed and plotted versus time. The slope of the graphs was then used to calculate the half-life of cyclin B. The dashed line indicated by an arrowhead represents the predicted graph for a protein with a half-life equal to the length of the cell cycle.

determine if phosphorylation is necessary or dispensable for their interaction and for cyclin B degradation. That staurosporine and calyculin A affect the phosphorylation of cyclin B interacting proteins and not the phosphorylation of cyclin B itself, suggests that phosphoregulation of cyclin B is indirect.

Since staurosporine prevents cells from entering mitosis and *Giardia* cyclin B is degraded during mitosis, we propose that staurosporine does not inhibit cyclin B degradation per se, but rather causes cells to accumulate at a stage in the cell cycle prior to mitotic onset where cyclin B levels are maintained at high levels (Fig. 8B). In contrast, calyculin A prevents mitotic exit, as cells proceed, then arrest in late anaphase with partially formed spindles, yet do not undergo cytokinesis. Untreated cells have no detectable levels of cyclin B once in anaphase or cytokinesis (supplementary material Fig. S3), yet cells treatment with calyculin A stabilizes cyclin B and arrests cells during anaphase. At this point in the cell cycle we would predict cyclin B degradation should be complete (depicted in Fig. 8B). Since cyclin B is stabilized in the presence of calyculin A we conclude that this drug inhibits cyclin B degradation. Our data also indicate that the phosphorylation of *Giardia* cyclin B, at least on threonine residues, is unaffected by either drug treatment. Several proteins that interact with cyclin B are phosphorylated and this phosphorylation correlates with increased stability of *Giardia* cyclin B. None of these cyclin B interacting bands could be stained using the MPM2 antibody suggesting that the phosphopeptides do not correspond to a T-P-x-K/R motif. It is unclear if these proteins bind to cyclin B irrespective of their phosphorylation status or if their phosphorylation is required for cyclin B binding.

Discussion

Due to its presence in most eukaryotic lineages, it has been suggested that the last eukaryotic common ancestor (LECA) had an APC/C. This implies that ubiquitination is an ancestral feature of eukaryotic cell cycle regulation (Eme et al.). *Giardia intestinalis* lacks an obvious APC. It is possible that *Giardia* has an APC so divergent as to be unrecognizable by current phylogenetic approaches (Eme et al., 2011). However, we show that *Giardia* cyclin B is highly atypical with regards to its regulation, and appears to be degraded independently of ubiquitination. In addition, other APC substrates, the aurora and polo-like kinases, also were not ubiquitinated. These observations suggest that *Giardia*, indeed, lacks an APC. This may reflect an evolutionarily divergence, or a cell cycle that predates the evolution of the APC.

While diverged in regulation, the function of *Giardia* cyclin B is similar to mitotic cyclins in other eukaryotes: it is required for mitotic entry, its levels oscillate during the cell cycle and it interacts with Cdk1 to form an active complex.

Overexpression of the cyclin B/Cdk inhibitor Sic1p together with deletion of Pds1 (Securin) and Clb5 (Shirayama et al., 1999; Thornton and Toczyski, 2003) allows budding yeast to bypass the need for APC-mediated degradation of cyclin B demonstrating that it is feasible to have a cell cycle with no APC. We cannot identify orthologues of securin, Sic1 or Clb5 in *Giardia*. We

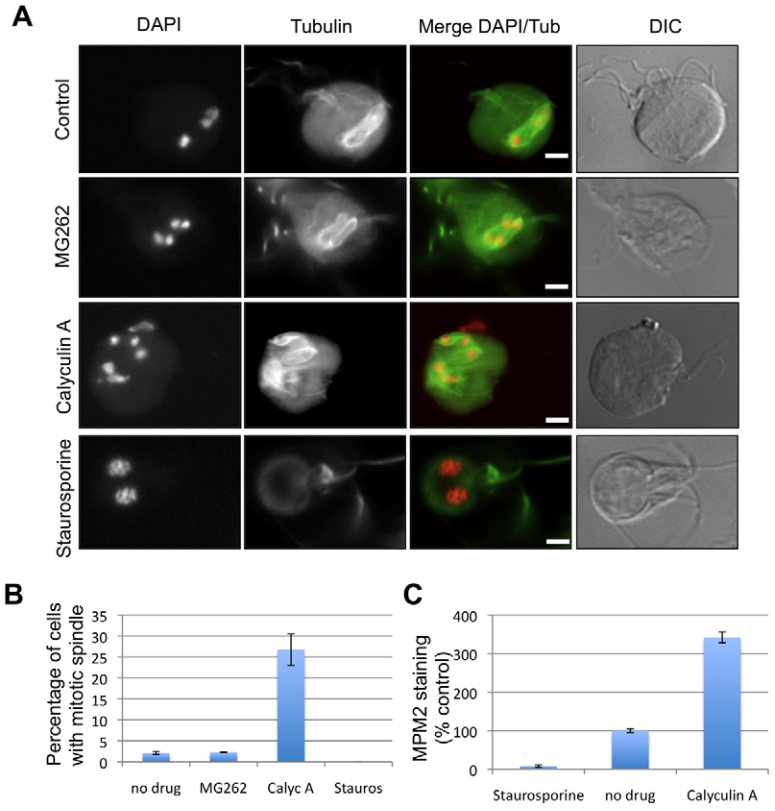

Fig. 6. Calyculin A and staurosporine inhibit cell cycle progression. (**A**) Cells treated with indicated drugs (15 hours, calyculin A 1 μM, staurosporine 0.1 μM, or DMSO for control) were fixed and stained for tubulin, actin and DNA and then photographed. DNA and tubulin signals were merged to show the mitotic spindle. For the untreated cells, a typical mitotic cell is shown for comparison. Scale bars: 2 μm. (**B**) Cells from A were scored for presence or absence of mitotic spindle and the results plotted. (**C**) Cells treated with staurosporine or calyculin A were lysed and analyzed by SDS-PAGE followed by immunoblotting using the MPM2 antibody. MPM2-specific signal was quantified and plotted as indicated.

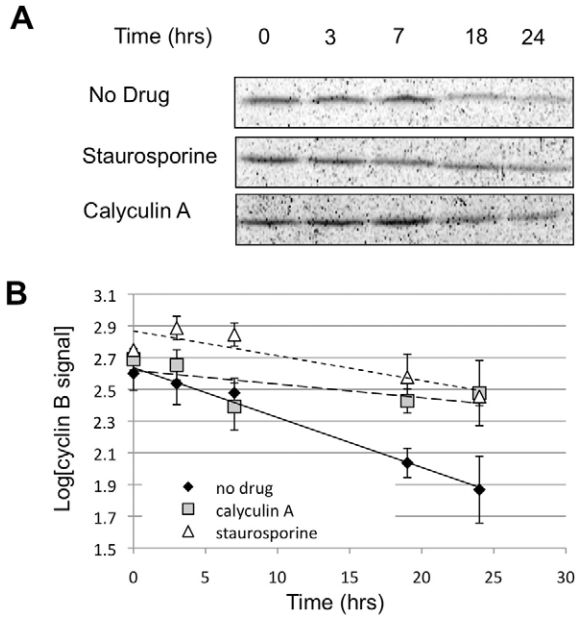

Fig. 7. Effects of calyculin A and staurosporine on cyclin B degradation. (**A**) Cells expressing SNAP-tagged cyclin B were labeled with SNAP-fluorescein, then incubated in the presence of drugs (for the time indicated, calyculin A 1 μM, staurosporine 0.1 μM, or DMSO for control) during the non-fluorescent chase. After the indicated time, cells were lysed and the fluorescence quantified. (**B**) Fluorescent signals from duplicates were log transformed and plotted versus time. The slope of the graphs was then used to calculate the half-life of cyclin B.

believe that the *Giardia* cell cycle network uses a distinct mechanism to bypass APC function as engineered yeast strains lacking the APC are extremely sick in contrast to the robust cell cycle observed in wild-type *Giardia*.

Our results in *Giardia* are the first description of an organism with a mitotic cyclin that is degraded independently of the APC. Indeed, cyclin degradation may be independent of ubiquitination. Our analysis suggests that the SCF complex (Skp1, Cullin, F-box), a separate multi-enzyme ubiquitin conjugation complex that coordinates cell cycle protein destruction (Skowyra et al., 1997; Lyapina et al., 1998), is also missing from *Giardia*. The proteasome inhibitor MG262 did not cause cell cycle arrest or appearance of higher molecular weight bands suggesting that no ubiquitin ligases (APC or SCF) are involved in cell cycle regulation in *Giardia*.

Ubiquitin conjugation allows for rapid protein degradation that is tightly linked to changes in the cell cycle and regulated by checkpoints. In *Giardia*, the half-life of cyclin B as determined by the pulse chase experiments is relatively long, compared to the short half-life of cyclin B observed in other organisms that have an APC. *Giardia* cells spend most of their cell cycle in the G2/M and S phases of the cell cycle (when combined these represent 85% of all cells in an asynchronously growing population); during both of these phases our data suggests cyclin B levels are high. Consequently, the relatively long half life of cyclin B could be due to the long time *Giardia* cells spend in phases of the cell cycle where cyclin B levels are high (S and G2/M). Our data show the half-life of cyclin B (8.8 hours) is notably less than the cell cycle length (14.1 hours); thus, although we cannot

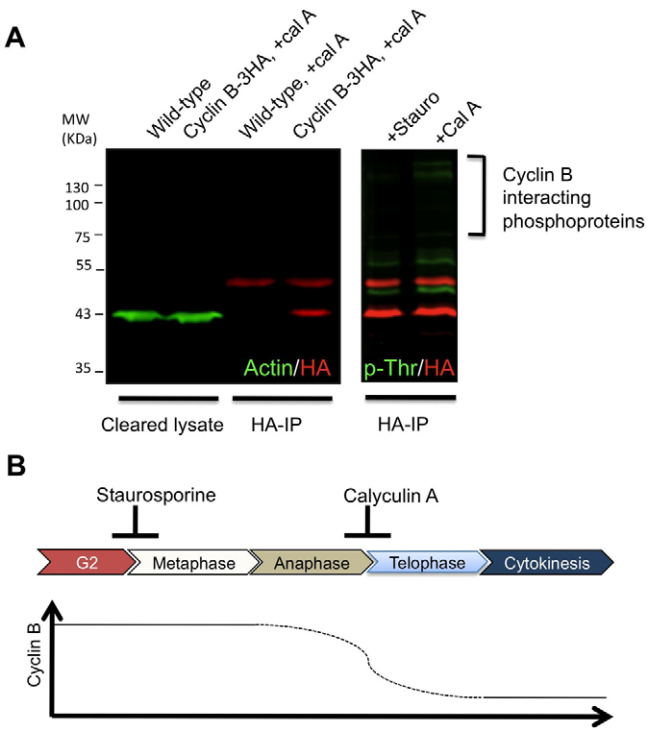

Fig. 8. Effects of calyculin A and staurosporine on cyclin B phosphorylation. (**A**) 3HA-tagged cyclin B was purified from cells treated with calyculin A or staurosporine by immunoprecipitation and probed using anti-HA to detect tagged *Giardia* cyclin B, anti-actin or anti-phospho-threonine (as indicated). Wild-type (untransfected) cells were used as a negative control to verify absence of nonspecific staining or binding to the HA purification matrix. The nonspecific ~50 kDa band present on the HA channel is caused by the IgG heavy chain from the purification matrix. Actin was used as loading control and to verify that proteins not bound to cyclin B were removed. (**B**) Model of how staurosporine and calyculin A affect cyclin B degradation. See text for further details.

completely rule out a role for division and subsequent dilution in reducing cyclin B levels after mitosis, our data are more consistent with a model where cyclin B is rapidly degraded during mitosis using an APC and ubiquitin independent mechanism. Our immunofluorescence data suggests that cyclin B in *Giardia* disappears promptly during mitotic onset and is degraded by the time cells complete anaphase. There is little change in cell volume between the onset of anaphase and cytokinesis in *Giardia*.

It has been suggested that the degradation of cyclins underwent permutations during evolution (Murray, 2004): initially cyclins were not degraded, but simply diluted as the cells divide. Later, the degradation of cyclins was linked to mitosis and to the activity of Cdk, other kinases and degradation-promoting complexes such as the APC or SCF. The evolution of these multi-protein ubiquitin ligases may have enabled a more rapid, adjustable and coordinated turnover of cell cycle regulatory proteins.

We hypothesize that cyclin B in *Giardia* is degraded during mitosis by a novel mechanism, involving interaction with one or more interacting proteins. We propose a model in which cyclin B in *Giardia* is targeted for degradation during mitosis not by the APC and ubiquitin conjugation, but by phosphorylation. A simple and elegant model is phosphorylation of cyclin B itself, by Cdk1 or another cell cycle regulatory kinase, regulates its degradation. However, we have not been able to detect any evidence of cyclin B phosphorylation. Alternatively, phosphorylation of cyclin B interactors could regulate cyclin B degradation, via two distinct mechanisms. The unknown cyclin B interactor could be binding cyclin B to promote its degradation. Phosphorylation of this interactor would inhibit its activity and consequently cyclin B degradation. Alternatively, the phosphorylation of an interactor could drive association with cyclin B thus protecting it from degradation. Currently, we are attempting to identify and characterize these unknown interactors.

Our findings raise many questions concerning cell cycle regulation in *Giardia*, including not only the mechanism of regulation of cyclin B turnover but also other substrates of the SCF or APC found in *Giardia*, that are involved in critical processes such as regulation of S phase, sister chromatid cohesion, and the spindle assembly checkpoint. We think it is unlikely that the absence of an APC is an adaptation to *Giardia*'s parasitic life style. Intracellular parasites, such as *Toxoplasma gondii*, have a functional APC and degradation sequences on their mitotic cyclins; and conversely other non-parasitic Diplomonads such as *Spironucleus vortens*, lack all APC components. Our results raise the question of whether the APC was present in the LECA and was lost by the POD group during their evolution or whether the APC evolved after the divergence of the POD group from other eukaryotes. If the latter is true, then the cell cycle in the LECA did not use ubiquitination to regulate cell cycle progression. This must remain an open question for now since its resolution is dependent on how phylogenomic trees of eukaryotic life are rooted (Fritz-Laylin et al., 2010).

Materials and Methods

Yeast assays

Cdc13-100 strain was obtained from the Yeast Genetic Resource Center Japan (http://yeast.lab.nig.ac.jp/nig/index_en.html). For experiments using GFP-tubulin, plasmids were transformed in strain FL52 (a gift from Dr Fei Li). Fission yeast strain h972- was used in all other experiments. The gene for cyclin B (accession GL50803_3977) was amplified by PCR to introduce a 5′ *Nde*I site and a 3′ *Sma*I site. The *Nde*I/*Sma*I cyclin B fragment and a *Sma*I/*Bam*HI fragment carrying the 3 myc tag [from vector pKS-3Myc-BSR (Gourguechon and Cande, 2011)] were cloned into *Nde*I and *Bam*HI sites of pRep42. The resulting pRep42-cyclinB vector was transformed into fission yeast by electroporation. To construct the pRep42-cyclinB-Ncdc13, an NdeI fragment of fission yeast cdc13p was cloned in frame upstream of the cyclin B gene. Yeast cells were grown at 30℃ for 3–4 days. For growth assays, cells were diluted in tenfold increments and spotted onto both – and + thiamine plates. To visualize yeast cells by fluorescence, cells were fixed in 70% ethanol for 30 minutes, permeabilized with phosphate-buffered saline/0.1% Triton X-100 and stained with DAPI.

Microscopy

Cells were mounted in Prolong antifade with DAPI reagent (Invitrogen), and examined using a Zeiss Axiovert 200M inverted fluorescence microscope using a 100× Zeiss oil immersion lens; data was acquired using the MetaMorph software (Molecular Devices); further image processing such as color merges was performed using ImageJ (NIH).

Cyclin B assays in *Giardia*

The *Giardia* strain carrying an integrated 3HA tagged cyclin B allele was used (Gourguechon and Cande, 2011). For morpholino-mediated knockdown, the sequence of cyclin B was submitted to the Gene Tools LLC website (www.gene-tools.com) to design and obtain oligos. A control oligo to control for nonspecific effects was also obtained by introducing six mismatches in the central region of the oligo. Morpholino oligos were used at 100 µM as previously described (Carpenter and Cande, 2009). At 24 hours after transfection cells were harvested and either lysed and analyzed by western blotting or fixed for immunofluorescence. For western blots, cells were harvested, lysed in Laemmli SDS sample buffer, resolved on a 10% acrylamide gel that was then transferred to a non-fluorescent PVDF

membrane and probed using anti-HA (HA-7, Sigma, 1:3000), anti-MPM2 (MPM2, Millipore, 1:1000) or anti-actin (Paredez et al., 2011) (1:3000), followed by fluorescent secondary antibody (IRDye680-linked anti-mouse and IRDye800-linked anti-rabbit, Li-Cor). Signals were detected and quantified using the Odissey infrared imager. For immunofluorescence, cells were fixed with 2% paraformaldehyde for 20 minutes, permeabilized with 0.5% Triton X-100 for 5 minutes, then stained using anti-HA antibody (followed by Alexa-Fluor-488-linked anti-mouse secondary, Invitrogen) and DAPI and examined for localization of cyclin B-3HA. To determine the size distribution of cyclin B depleted cells, cells were additionally treated with Sypro Ruby to stain the entire cell and ~500 cells were analyzed using the CellProfiler program (www.cellprofiler.org) (Carpenter et al., 2006). The distribution of size or cyclin B 3HA levels, depending on the experiment was plotted on a histogram.

Quantitative cytometry assays

To quantify cyclin B levels in the cell population, 102 images (both FITC and DAPI channels) were taken for untransfected, cyclin B 3HA cells transfected with mismatch oligos and cyclin B 3HA cells transfected with anti-cyclin B morpholino. The CellProfiler program was used to analyze ~4000 cells per data set. Each image was corrected for intensity of DNA as previously described (Jones et al., 2008), by taking the log of integrated DAPI staining of each nuclei and setting it at a value of 2. This was done to correct the small (one- to twofold) variation of intensity from image to image. For each cell, a value of integrated DNA intensity and integrated cyclin B intensity was generated. Cells were then categorized according to their nuclear DNA content as G1 (4N), S (4–8N) or G2/M (8N). For each category of cells a histogram of integrated cyclin B 3HA staining per cell was generated. Cells not transfected with the cyclin B 3HA construct were also analyzed and their cyclin B staining used to define background levels of immunofluorescence. Background was subtracted from all experimental values.

Ubiquitination assays

Cell lines were constructed, using previously described methods (Gourguechon and Cande, 2011), to express a 3HA-tagged allele of AUK (accession GL50803_5358) or PLK (accession GL50803_104150). These cells were then incubated for 12 hours in the presence, or absence, of the proteasomal inhibitor MG262 (5 μM, Boston Biochemicals), then lysed in PBS pH 7.4 supplemented with Halt protease inhibitors (Thermo Fisher scientific). Ubiquitin-conjugated proteins were then affinity purified using the UbiQapture kit (Enzo life sciences) according to the manufacturer's instructions and analyzed by anti-ubiquitin (provided with the UbiQapture kit), anti-actin or anti-HA western blotting (using HRP-linked anti-mouse and anti-rabbit, secondary antibodies, Bio-Rad; blots were stripped between blots using Restore stripping reagent, Thermo Fisher scientific).

Pulse chase degradation assays

The 3HA tag in pcCycB3HAPAC (Gourguechon and Cande, 2011) was replaced with the SNAP tag from pSNAPf (New England Biolabs) and the resulting vector, verified, linearized with NruI and transfected into *Giardia* cells as described. Cells expressing SNAP-tagged cyclin B (~1×10^8 cells) were iced and harvested, then incubated in 1 ml of complete media containing 5 μM of SNAP-fluorescein (New England Biolabs) for 3 hours at 37℃. Cells were chilled on ice for 20 minutes, harvested by centrifugation and resuspended in fresh media containing 10 μM SNAP-Block reagent (New England Biolabs) to start the chase. Inhibitors of the proteasome (MG262, 5 μM), phosphatases PP1 and PP2 (1 μM calyculin A, Cell Signaling Technologies) or kinases (0.2 μM staurosporine, Millipore) were added as indicated. Cells were then harvested at each timepoint (0, 3, 7, 18, 25 hours) by chilling on ice for 20 minutes, centrifugation and resuspension in 50 μl of 1× Laemmli SDS sample buffer. The quantity of protein for each sample was determined using the Dc protein assay system (Bio-Rad) to allow equal loading of proteins on the gel. For each timepoint, duplicate samples were taken. Samples were analyzed by SDS PAGE followed by imaging using a Typhoon fluorescent scanner (GE Biosciences). Results were log10 transformed, and the mean of the duplicates plotted versus time and the slope of the trendline determined, then used to calculate the half-life. Error bars were generated using the standard deviation between the duplicate samples.

Phosphorylation assays of cyclin B

Cells expressing 3HA tagged cyclin B were untreated, treated with 1 μM calyculin A or 0.2 μM staurosporine as indicated, then lysed under native conditions and HA-tagged proteins immunoprecipitated as previously described, then analyzed by western blotting using a rabbit anti-phosphothreonine antibody (Cell Signaling Technologies, #9381). Anti-HA and anti-actin antibodies were used as described to confirm the presence of cyclin B and equal loading.

Histone kinase assay

Immunoprecipitated cyclin B 3-HA was incubated with 5 μg of bovine histone H1 and 2 μCi of γ-[^{32}P]ATP together with 25 μM cold ATP for 20 minutes at 23℃ in kinase assay buffer containing 150 mM NaCl, 25 mM HEPES pH 7.5, 10 mM Mg^{2+} and 1 mM DTT. Reactions were stopped by adding SDS sample buffer and boiling, then analyzed by SDS PAGE followed by autoradiography, or Coomassie Blue staining to stain for total histone H1.

Reporter gene assays

A region including 200 nucleotides 5′ of the cyclin B start codon was inserted into the pGFP-pac vector, replacing the promoter. A second region, including 100 nucleotides immediately 3′ to the cyclin B stop codon was inserted downstream of GFP. Thus, GFP was under the control of the cyclin B promoter and terminator sequences. This construct was transfected into *Giardia* WBC6 cells, as previously described. Transfected cells were selected using puromycin (10 μg/ml), then incubated for 30 minutes in pre-warmed PBS before fixation to allow proper, oxygen-dependent folding of GFP. Cells were then analyzed as in Fig. 3, to determine GFP and DNA content for each cell, categorized into G1, S or G2/M cells then plotted as a histogram for GFP staining as indicated. Cells not transfected were again used to define background levels, which were subtracted from experimental values.

Acknowledgements

We thank our colleagues for technical help and critical reading of this manuscript. Many thanks to Dr Fei Li for the FL52 yeast strain, Prof. Keith Gull for the anti-tubulin antibody and Magdalena Uzlikova for technical advice.

Author contributions

S.G. and W.Z.C. designed the research; S.G. and L.J.H. performed experiments and analysed the data; S.G., L.J.H. and W.Z.C. wrote the manuscript.

Funding

This work was supported by the National Institutes of Health [grant number A1054693 to W.Z.C.]. The funders had no role in study design, data collection and analysis, decision to publish, or preparation of the manuscript. Deposited in PMC for release after 12 months.

Supplementary material available online at
http://jcs.biologists.org/lookup/suppl/doi:10.1242/jcs.121632/-/DC1

References

Adam, R. D. (2001). Biology of Giardia lamblia. *Clin. Microbiol. Rev.* **14**, 447-475.
Bernander, R., Palm, J. E. and Svärd, S. G. (2001). Genome ploidy in different stages of the Giardia lamblia life cycle. *Cell. Microbiol.* **3**, 55-62.
Booher, R. and Beach, D. (1988). Involvement of cdc13+ in mitotic control in Schizosaccharomyces pombe: possible interaction of the gene product with microtubules. *EMBO J.* **7**, 2321-2327.
Brizuela, L., Draetta, G. and Beach, D. (1989). Activation of human CDC2 protein as a histone H1 kinase is associated with complex formation with the p62 subunit. *Proc. Natl. Acad. Sci. USA* **86**, 4362-4366.
Carpenter, M. L. and Cande, W. Z. (2009). Using morpholinos for gene knockdown in Giardia intestinalis. *Eukaryot. Cell* **8**, 916-919.
Carpenter, A. E., Jones, T. R., Lamprecht, M. R., Clarke, C., Kang, I. H., Friman, O., Guertin, D. A., Chang, J. H., Lindquist, R. A., Moffat, J. et al. (2006). CellProfiler: image analysis software for identifying and quantifying cell phenotypes. *Genome Biol.* **7**, R100.
Ciccarelli, F. D., Doerks, T., von Mering, C., Creevey, C. J., Snel, B. and Bork, P. (2006). Toward automatic reconstruction of a highly resolved tree of life. *Science* **311**, 1283-1287.
Davids, B. J., Williams, S., Lauwaet, T., Palanca, T. and Gillin, F. D. (2008). Giardia lamblia aurora kinase: a regulator of mitosis in a binucleate parasite. *Int. J. Parasitol.* **38**, 353-369.
Draetta, G., Luca, F., Westendorf, J., Brizuela, L., Ruderman, J. and Beach, D. (1989). Cdc2 protein kinase is complexed with both cyclin A and B: evidence for proteolytic inactivation of MPF. *Cell* **56**, 829-838.
Eme, L., Trilles, A., Moreira, D. and Brochier-Armanet, C. (2011). The phylogenomic analysis of the anaphase promoting complex and its targets points to complex and modern-like control of the cell cycle in the last common ancestor of eukaryotes. *BMC Evol. Biol.* **11**, 265.
Fang, G., Yu, H. and Kirschner, M. W. (1999). Control of mitotic transitions by the anaphase-promoting complex. *Philos. Trans. R. Soc. B* **354**, 1583-1590.
Fritz-Laylin, L. K., Prochnik, S. E., Ginger, M. L., Dacks, J. B., Carpenter, M. L., Field, M. C., Kuo, A., Paredez, A., Chapman, J., Pham, J. et al. (2010). The genome of Naegleria gruberi illuminates early eukaryotic versatility. *Cell* **140**, 631-642.
Gallego, E., Alvarado, M. and Wasserman, M. (2007). Identification and expression of the protein ubiquitination system in Giardia intestinalis. *Parasitol. Res.* **101**, 1-7.

Geley, S., Kramer, E., Gieffers, C., Gannon, J., Peters, J. M. and Hunt, T. (2001). Anaphase-promoting complex/cyclosome-dependent proteolysis of human cyclin A starts at the beginning of mitosis and is not subject to the spindle assembly checkpoint. *J. Cell Biol.* **153**, 137-148.

Gourguechon, S. and Cande, W. Z. (2011). Rapid tagging and integration of genes in Giardia intestinalis. *Eukaryot. Cell* **10**, 142-145.

Hammarton, T. C., Clark, J., Douglas, F., Boshart, M. and Mottram, J. C. (2003). Stage-specific differences in cell cycle control in Trypanosoma brucei revealed by RNA interference of a mitotic cyclin. *J. Biol. Chem.* **278**, 22877-22886.

Hershko, A., Ganoth, D., Sudakin, V., Dahan, A., Cohen, L. H., Luca, F. C., Ruderman, J. V. and Eytan, E. (1994). Components of a system that ligates cyclin to ubiquitin and their regulation by the protein kinase cdc2. *J. Biol. Chem.* **269**, 4940-4946.

Jones, T. R., Kang, I. H., Wheeler, D. B., Lindquist, R. A., Papallo, A., Sabatini, D. M., Golland, P. and Carpenter, A. E. (2008). CellProfiler Analyst: data exploration and analysis software for complex image-based screens. *BMC Bioinformatics* **9**, 482.

King, R. W., Peters, J. M., Tugendreich, S., Rolfe, M., Hieter, P. and Kirschner, M. W. (1995). A 20S complex containing CDC27 and CDC16 catalyzes the mitosis-specific conjugation of ubiquitin to cyclin B. *Cell* **81**, 279-288.

Kumar, P. and Wang, C. C. (2005). Depletion of anaphase-promoting complex or cyclosome (APC/C) subunit homolog APC1 or CDC27 of Trypanosoma brucei arrests the procyclic form in metaphase but the bloodstream form in anaphase. *J. Biol. Chem.* **280**, 31783-31791.

Lauwaet, T., Davids, B. J., Torres-Escobar, A., Birkeland, S. R., Cipriano, M. J., Preheim, S. P., Palm, D., Svärd, S. G., McArthur, A. G. and Gillin, F. D. (2007). Protein phosphatase 2A plays a crucial role in Giardia lamblia differentiation. *Mol. Biochem. Parasitol.* **152**, 80-89.

Li, Y., Li, Z. and Wang, C. C. (2003). Differentiation of Trypanosoma brucei may be stage non-specific and does not require progression of cell cycle. *Mol. Microbiol.* **49**, 251-265.

Lyapina, S. A., Correll, C. C., Kipreos, E. T. and Deshaies, R. J. (1998). Human CUL1 forms an evolutionarily conserved ubiquitin ligase complex (SCF) with SKP1 and an F-box protein. *Proc. Natl. Acad. Sci. USA* **95**, 7451-7456.

Marks, J., Hagan, I. M. and Hyams, J. S. (1986). Growth polarity and cytokinesis in fission yeast: the role of the cytoskeleton. *J. Cell Sci. Suppl.* **5**, 229-241.

Morrison, H. G., McArthur, A. G., Gillin, F. D., Aley, S. B., Adam, R. D., Olsen, G. J., Best, A. A., Cande, W. Z., Chen, F., Cipriano, M. J. et al. (2007). Genomic minimalism in the early diverging intestinal parasite Giardia lamblia. *Science* **317**, 1921-1926.

Murray, A. W. (2004). Recycling the cell cycle: cyclins revisited. *Cell* **116**, 221-234.

Mutomba, M. C., To, W. Y., Hyun, W. C. and Wang, C. C. (1997). Inhibition of proteasome activity blocks cell cycle progression at specific phase boundaries in African trypanosomes. *Mol. Biochem. Parasitol.* **90**, 491-504.

Nohýnkova, E., Dráber, P., Reischig, J. and Kulda, J. (2000). Localization of gamma-tubulin in interphase and mitotic cells of a unicellular eukaryote, Giardia intestinalis. *Eur. J. Cell Biol.* **79**, 438-445.

Paredez, A. R., Assaf, Z. J., Sept, D., Timofejeva, L., Dawson, S. C., Wang, C. J. and Cande, W. Z. (2011). An actin cytoskeleton with evolutionarily conserved functions in the absence of canonical actin-binding proteins. *Proc. Natl. Acad. Sci. USA* **108**, 6151-6156.

Paugam, A., Bulteau, A. L., Dupouy-Camet, J., Creuzet, C. and Friguet, B. (2003). Characterization and role of protozoan parasite proteasomes. *Trends Parasitol.* **19**, 55-59.

Peters, J. M. (2006). The anaphase promoting complex/cyclosome: a machine designed to destroy. *Nat. Rev. Mol. Cell Biol.* **7**, 644-656.

Poxleitner, M. K., Dawson, S. C. and Cande, W. Z. (2008). Cell cycle synchrony in Giardia intestinalis cultures achieved by using nocodazole and aphidicolin. *Eukaryot. Cell* **7**, 569-574.

Regoes, A. and Hehl, A. B. (2005). SNAP-tag mediated live cell labeling as an alternative to GFP in anaerobic organisms. *Biotechniques* **39**, 809-810, 812.

Reiner, D. S., Ankarklev, J., Troell, K., Palm, D., Bernander, R., Gillin, F. D., Andersson, J. O. and Svärd, S. G. (2008). Synchronisation of Giardia lamblia: identification of cell cycle stage-specific genes and a differentiation restriction point. *Int. J. Parasitol.* **38**, 935-944.

Riabowol, K., Draetta, G., Brizuela, L., Vandre, D. and Beach, D. (1989). The cdc2 kinase is a nuclear protein that is essential for mitosis in mammalian cells. *Cell* **57**, 393-401.

Sagolla, M. S., Dawson, S. C., Mancuso, J. J. and Cande, W. Z. (2006). Three-dimensional analysis of mitosis and cytokinesis in the binucleate parasite Giardia intestinalis. *J. Cell Sci.* **119**, 4889-4900.

Shirayama, M., Tóth, A., Gálová, M. and Nasmyth, K. (1999). APC(Cdc20) promotes exit from mitosis by destroying the anaphase inhibitor Pds1 and cyclin Clb5. *Nature* **402**, 203-207.

Skowyra, D., Craig, K. L., Tyers, M., Elledge, S. J. and Harper, J. W. (1997). F-box proteins are receptors that recruit phosphorylated substrates to the SCF ubiquitin-ligase complex. *Cell* **91**, 209-219.

Thornton, B. R. and Toczyski, D. P. (2003). Securin and B-cyclin/CDK are the only essential targets of the APC. *Nat. Cell Biol.* **5**, 1090-1094.

Westendorf, J. M., Rao, P. N. and Gerace, L. (1994). Cloning of cDNAs for M-phase phosphoproteins recognized by the MPM2 monoclonal antibody and determination of the phosphorylated epitope. *Proc. Natl. Acad. Sci. USA* **91**, 714-718.

Whitfield, W. G., Gonzalez, C., Maldonado-Codina, G. and Glover, D. M. (1990). The A- and B-type cyclins of Drosophila are accumulated and destroyed in temporally distinct events that define separable phases of the G2-M transition. *EMBO J.* **9**, 2563-2572.

Yamano, H., Gannon, J. and Hunt, T. (1996). The role of proteolysis in cell cycle progression in Schizosaccharomyces pombe. *EMBO J.* **15**, 5268-5279.

Yamano, H., Tsurumi, C., Gannon, J. and Hunt, T. (1998). The role of the destruction box and its neighbouring lysine residues in cyclin B for anaphase ubiquitin-dependent proteolysis in fission yeast: defining the D-box receptor. *EMBO J.* **17**, 5670-5678.

Yu, H., King, R. W., Peters, J. M. and Kirschner, M. W. (1996). Identification of a novel ubiquitin-conjugating enzyme involved in mitotic cyclin degradation. *Curr. Biol.* **6**, 455-466.

Journal of Cell Science